A Maximum Power Point Tracker using Positive Feedforward Control based on the DC Motor Dynamics and PVM Mathematical Model

Jesus Gonzalez-Llorente*, Eduardo I. Ortiz-Rivera† and Andres Diaz‡
Department of Electrical and Computer Engineering
University of Puerto Rico at Mayaguez
PO Box 9042, Mayaguez, PR 00681-9042
Email: *jesus.gonzalez@ece.uprm.edu, †eduardo.ortiz@ece.uprm.edu, ‡ajdiaz@uprm.edu

***Abstract*—This paper presents a maximum power tracking method for DC motor fed from photovoltaic modules (PVM) through step-down power converter. This method employs positive feedback of motor speed; therefore, only DC motor speed measurements are required. The designed control law is based on mathematical model of DC motor and power converter, and also, variations of optimal maximum power point (MPP) are considered at different values of irradiance. Optimal MPP is approximated by method known as linear reoriented coordinates method (LRCM). Finally, a simple analog circuit is designed and implemented, which calculates optimal duty ratio for power converter according to DC motor speed.**

I. INTRODUCTION

There are many applications today in which photovoltaic (PV) modules can be used, in particular small off grid loads, such as basic lighting, refrigeration, telecommunications and water pumping [1]. In some of these cases, a DC motor is connected to a PV module as load [2].

The power (P) delivered by a PVM will be a function of ambient conditions, as well as of the load that the PVM are supplying [2]. For most of DC motor directly connected to PVM, the operating point, which is given by intersection of PV and DC motor $I-V$ curves, is very far from the maximum power point (MPP) of the PVM [2]–[4].

In order to improve the performance, the equilibrium operating point must be closer to MPP of PVM via matching of DC motor to PVM. The matching could be reached in two ways. First, without interfacing circuit, selecting carefully a DC motor according to motor I-V curve, mechanical load characteristics and PVM parameters [5]–[7]. Second, by including an electronic control device, known as maximum power point tracker (MPPT), which continuously matches the output characteristics of the PVM to the input characteristics of the motor [3], [4], [8], [9].

In [10]–[14] step-down DC-DC power converters were used as circuit interface for matching a PVM with a DC motors; but, none of them specifics necessary conditions for optimal matching with step-down converter. In addition, the research [13], [14] assert that they could match a PVM with a DC motor as well as regulating the speed.

In this paper, based on the DC motor dynamics and the PVM mathematical model, a positive feedback of speed is derived to track the maximum power point of a PVM that is supplying a permanent magnet DC motor though a step-down converter. The effect of a proportional speed load is also analyzed and the load conditions to reach matching is found.

The paper is divided into five parts. First section presented the introduction. Second section describes how the analyzed system is modeled: a exponential model, which was proposed in [15] is used to describe the PVM behavior, the DC motor is modeled using differential equations and the chopper output-input relationship is used to describe the behavior of power converter.

In third section, the procedure to derive the control law is described. Mathematical analysis is used to derive a relationship between optimal duty ratio and motor speed in steady state conditions. The applied method to approximate the PVM optimal voltage and the optimal current is called Linear Reoriented Coordinates Method (LRCM). This method was proposed in [16].

In next section, the characteristics of real DC motor and the PVM parameters are identified and showed. Besides, this section shows software simulation and experimental results for different irradiance values. Finally, conclusions are presented.

II. DESCRIPTION AND MODELING OF THE SYSTEM

The analyzed system consists of a photovoltaic array, a step-down chopper converter and a DC motor in its power circuit. This system is shown in Fig 1.

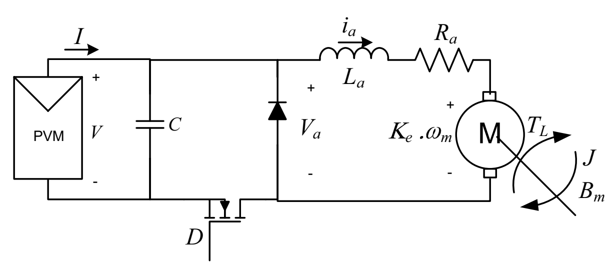

Fig. 1. PV system supplying a DC motor through step-down converter

A. PVM Model Description

The relationship of the current (I) with respect to the voltage (V), for any PV array is given in (1) and can be described in terms of the values provided by the manufacturer's data sheet and the standard test conditions (STC).

This model takes into consideration the short-circuit current (I_x) and the open-circuit voltage (V_x) at any given irradiance level (E_i) and temperature (T), the PVM characteristic constant (b), and the numbers of in series and in parallels modules with the same electrical characteristics (s and p, respectively). The PVM exponential model is fully described in [15], [17].

$$I(V) = \frac{p \cdot Ix}{1 - exp\left(\frac{-1}{b}\right)} \cdot \left[1 - exp\left(\frac{V}{b \cdot s \cdot Vx} - \frac{1}{b}\right)\right] \quad (1)$$

The constant b can be calculated using an algorithm based on the Fixed Point Theorem. The algorithm is given by (2), where ξ is the maximum permitted error, V_{oc} and I_{sc} are open-circuit voltage and short-circuit current at STC, V_{op} and I_{op} are optimal voltage and optimal current at STC.

$$\begin{array}{l} \text{while}|b_{n+1} - b_n| > \xi \\ b_{n+1} = \frac{V_{op} - V_{oc}}{V_{oc} \cdot \ln\left[1 - \frac{I_{op}}{I_{sc}} \cdot \left(1 - \exp\frac{1}{b_n}\right)\right]} \end{array} \quad (2)$$

B. DC Motor Model

Electrical side of DC motor can be described for (3), and the torque balance equation is given by (4)

$$V_a = R_a \cdot i_a + L_a \frac{di_a}{dt} + K_e \cdot \omega_m \quad (3)$$

$$T_e = J \cdot \frac{d\omega_m}{dt} + B_m \cdot \omega_m + T_L \quad (4)$$

In the above equations R_a, L_a, K_e, V_a and i_a are armature resistance, armature inductance, back emf constant, armature voltage and current respectively. J, B_m, and T_L are the moment of inertia of the motor and connected load, constant viscous friction coefficient and load torque, respectively.

The electromagnetic torque, T_e, is proportional to the current through the armature winding and can be written as $T_e = K_e \cdot i_a$. In this paper the motor is loaded through an eddy current brake and the load torque-speed characteristics is given by $T_L = c_1 \cdot \omega_m + c_2$, where c_1 and c_2 are constants whose values depend on position of the braking magnet.

C. Chopper Converter Model

Chopper produces a lower average output voltage, V_o, than d.c. input voltage, V_i. The averaged equations for the chopper are:

$$I_o = I_i / D \quad (5)$$

$$V_o = D \cdot V_i \quad (6)$$

Where D is the duty ratio, and I_0 and I_i are output current and input current respectively.

III. Control law derivation

A. Optimal duty ratio

Using the buck chopper converter, the duty ratio is expressed by $D = V_o/V_i$. In the system shown in Fig 1, the power converter output voltage V_o is equal to the motor armature voltage, V_a. The power converter input voltage V_i is equal to PVM voltaje V, or equal to V_{op} if the terminal voltage of the PVM is operating in the maximum power point. Then, the optimal duty ratio is given by (7)

$$D = \frac{V_a}{V_{op}} \quad (7)$$

The optimal voltage, V_{op} can be derived by means of a maximum power point tracking method, which will be described below. The armature voltage V_a, is calculated by solution in steady state of (3); this is given by

$$V_a = R_a \cdot I_a + K_e \cdot \omega_m \quad (8)$$

Since $T_e = K_e \cdot i_a$, solving for current I_a of (4) in steady state condition, yields the expression:

$$I_a = (B_m \cdot \omega_m + T_L)/(K_e) \quad (9)$$

Therefore, substituting (9) into (8), we can get

$$V_a = R_a \left(\frac{B_m \cdot \omega_m + T_L}{K_e}\right) + K_e \cdot \omega_m \quad (10)$$

So, the optimal duty ratio becomes:

$$D = \frac{V_a}{V_{op}} = \frac{1}{V_{op}} \left[K_e \cdot \omega_m + R_a \left(\frac{B_m \cdot \omega_m + T_L}{K_e}\right)\right] \quad (11)$$

In order to obtain a relationship between the optimal duty ratio and the maximum motor speed, we derive the last one from the power balance equation under steady state condition. This is:

$$P = I_a^2 \cdot R_a + E_a \cdot I_a \quad (12)$$

Knowing that $E_a \cdot I_a$ is the power in rotational motion, which is equal to the product of the torque and angular velocity, then the equation (12) becomes:

$$P = I_a^2 \cdot R_a + T_L \cdot \omega_m \quad (13)$$

Substituting (9) into (13) we can get the equation (14), which is used to calculate the DC motor speed when the power is known. If we assume that efficiency of power converter is 1 p.u., the motor power is equal to PVM power, which is obtained using the MPPT method.

$$\begin{array}{rcl} P & = & B_m \cdot \omega_m^2 + T_L \cdot \omega_m + \\ & & \left(B_m^2 \cdot \omega_m^2 + 2B_m \cdot \omega_m T_L + T_L^2\right) \frac{R_a}{K_e^2} \end{array} \quad (14)$$

B. Maximum power point tracking method

In order to obtain V_{op}, we use Linear Reoriented Coordinates Method (LRCM) [16]. This method approximates the optimal voltage V_{op}, the optimal current I_{op} and maximum power rating P_{max} using the same variables as the dynamic model.

The equations of the approximated optimal voltage, V_{ap} and the approximated optimal current I_{ap} are given by (15) and (16) respectively; then, the approximated P_{max} is given by the multiplication of V_{ap} and I_{ap} [16].

$$V_{ap} = V_x + b \cdot V_x \cdot ln\left(b - b \cdot exp(-\frac{1}{b})\right) \leq V_{op} \tag{15}$$

$$I_{ap} = I_x \cdot \frac{1 - b + b \cdot exp\left(\frac{-1}{b}\right)}{1 - exp\left(\frac{-1}{b}\right)} \geq I_{op} \tag{16}$$

C. Algorithm to find the control law

By substituting $T_L = c_1 \cdot \omega_m + c_2$ into equation (11) and reorganizing terms, we can note that the optimal duty ratio can be written as $D = A + B \cdot \omega_m$, where A and B are given by (17) and (18).

$$A = \frac{R_a \cdot c_2}{V_{op} \cdot K_e} \tag{17}$$

$$B = \frac{K_e}{V_{op}} + \frac{R_a(B_m + c_1)}{V_{op} \cdot K_e} \tag{18}$$

For different irradiance values, we can use the PVM model and the MPPT method described above, to find the maximum power, P_{max}, and the optimal voltage, V_{op}. Then, we calculate the motor speed using (14) and the armature voltage from (8). Afterwards, optimal duty ratio is calculated from (7). Finally, we must graph the optimal duty ratio against the motor speed, and the constants A and B can be calculated using curve fitting techniques.

D. Implementation of control law

We have showed that the optimal duty ratio has the form $D = A + B\omega_m$, as well as, the way to find the constant values A and B. Then, Fig. 2 shows how this law can be implemented. This configuration uses a tachometer, which generates a voltage, V_{th}, proportional to speed given by $V_{th} = K_{th} \cdot \omega_m$.

For a PWM generator, the duty ratio is given by $D = K_D \cdot v_c$, with $K_D = \frac{1}{V_{max}}$ and $v_c = V_{adj} + K_a \cdot v_{th}$. The variables V_{adj} and K_a are adjusted to obtain the A and B values according to (19); from which $A = K_D \cdot V_{adj}$ and $B = K_D \cdot K_a \cdot K_{th}$

$$D = K_D \cdot V_{adj} + K_D \cdot K_a \cdot K_{th} \cdot \omega_m \tag{19}$$

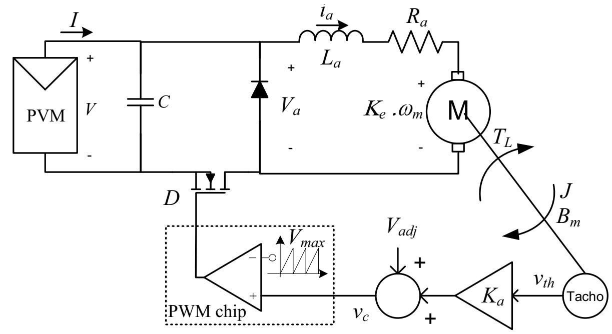

Fig. 2. Power circuit and control law schematic

TABLE I
PARAMETERS FOR PERMANENT MAGNET DC MOTOR

Symbol	Parameter	Value	Units
R_a	Armature resistance	8.57	Ω
L_a	Armature inductance	58.7	mH
K_e	Back emf constant	0.1485	$\frac{V}{rad/sec}$
J	Moment of inertia	45.5×10^{-6}	$Kg \cdot m^2$
B_m	Viscous friction coefficient	94.8×10^{-6}	$\frac{N \cdot m}{rad/seg}$

TABLE II
PVM BP SX10M SPECIFICATIONS AT STC

Symbol	Parameter	Value	Units
I_{sc}	Short-circuit Current	0.65	A
V_{oc}	Open-circuit Voltage	21.0	V
P_{max}	Maximum Power	10.0	W
V_{op}	Voltage at P_{max}	16.8	V
I_{op}	Current at P_{max}	0.59	A
TCi	Temperature coeff. of I_{sc}	(0.065 $\pm$0.015)	$\%/C$
TCv	Temperature coeff. of V_{oc}	-(80 $\pm$10)	mV/C

IV. RESULTS

The permanent magnet DC motor used has the parameter listed in table I [11]. The motor is loaded though an eddy current brake, where the position of the braking magnet define the load torque (T_L) applied. In this case the load torque is proportional to speed and it is given by $T_L = c_1 \cdot \omega_m + c_2$. The constants c_1 and c_2 are calculated from real data; so, for three different positions, we have the following torque-speed characteristics: $T_L = 0.00014\omega_m + 0.024$, $T_L = 0.00055\omega_m + 0.024$ and $T_L = 0.00074\omega_m + 0.023$.

The PV array used for this study consist of two PVM BP SX10M connected in series. The electrical characteristics of PVM BP SX10M are presented in table II. The PVM characteristic constant is $b = 0.084$; it was calculated using (2). Figs. 3 and 4 show the measured and simulated $I - V$ and $P - V$ characteristic curves for the PV array; the markers represent the measured data.

A. Calculation of control law

For different torque-speed characteristics, DC motor $P - V$ curves are superimposed on a set of PVM $P - V$ curves in Fig. 5. This shows that for DC motor operate at MPP, with $T_L = 0.00074\omega_m + 0.023$ or $T_L = 0.00055\omega_m + 0.02$, the motor

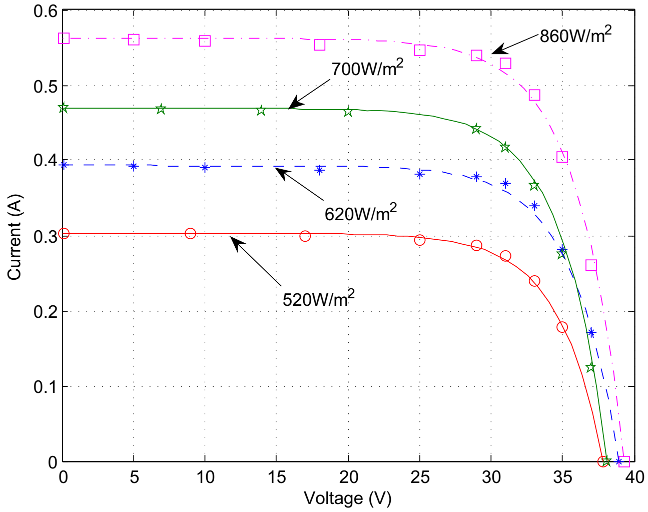

Fig. 3. I-V Characteristic of PV array

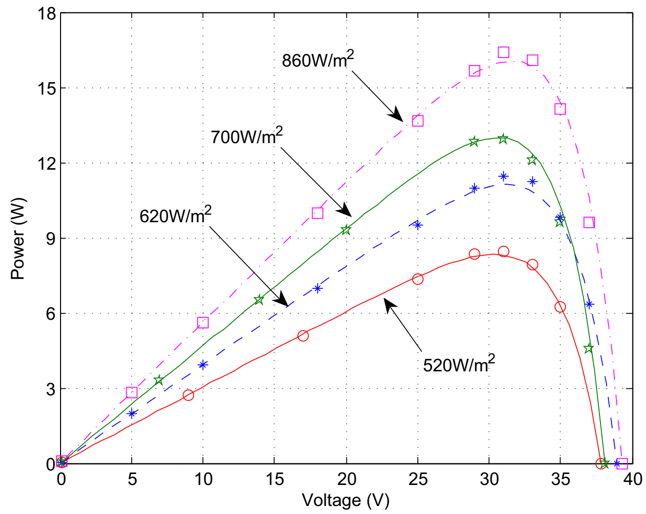

Fig. 4. P-V Characteristic of PV array

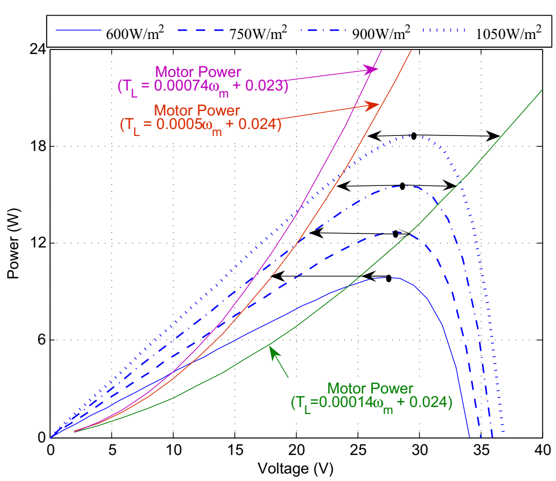

Fig. 5. Power curves DC motor and PVM

voltage must be lower that PVM voltage at MPP, therefore a step-down power converter, such as a chopper can be used.

Then, we chose the position of the braking magnet with torque-speed characteristic given by $T_L = 0.00055 \cdot \omega_m + 0.024$. For temperature of $59°C$, we obtained V_{ap}, I_{ap} and P_{max} by LRCM, motor speed, ω_m, at P_{max} using (14) and optimal duty ratio from (11) for different values of irradiance. Fig. 6 shows the variations of duty ratio D with ω_m, which describes the control law, it is given by $D = 0.0052 \cdot \omega_m + 0.2$.

B. Simulation results

The system was implemented in SABER® as is shown in Fig. 7. The PV array and the DC motor were modeled using the equations described in the section II and the parameters listed in tables I and II; while, the power converter was simulated using semiconductor switches.

The control law $D = 0.0052 \cdot \omega_m + 0.2$ was implemented using operational amplifier, selecting the resistance values to attain the specified gains. A PWM chip, with $K_D = 1/3$ was used to generate the signal to activate the MOSFET according to the output operational amplifiers. A tachometer with constant $K_{th} = 0.0191 \frac{V}{rad/seg}$ was used to sense the motor speed.

The simulation is done for irradiance values of 600 W/m^2, $1050 W/m^2$ and $900 W/m^2$. Fig. 8 shows the DC motor speed and the power of PVM, and Fig. 9 shows voltage and current of PVM. Table III summarizes the results comparing control and direct coupling.

TABLE III
SUMMARY RESULTS

E_i	PVM Power [W]		
$[W/m^2]$	in MPP	With Control	With Direct Coupling
600	9.88	9.83	4.86
900	15.61	15.49	12.52
1050	18.68	18.57	17.14

C. Experimental results

The experiment setup is similar to the simulated scheme, so this consists of the DC motor and the PVMs specified in tables I and II. The control law was implemented through a operational amplifiers (LM324) and a regulating pulse width modulator (PWM) chip (UC3526). The switching frequency was fixed to $10kHz$ with the external components connected to the PWM chip. The experiment setup is shown in Fig 13.

In the test condition, the PVM open-circuit voltage was $V_{oc} = 39.35V$ and the PVM short-circuit current was $I_{sc} = 0.71$, then, the estimated maximum power was $P_{max} = 20W$. Fig 10, 11 and 12 show the measured waveforms using a 10X probes.

Fig. 10 shows the PWM signal applied to the MOSFET gate, its duty ratio is $D = 0.73$, the measured DC motor speed was $\omega_m = 104.18 rad/s$; this result accords to the control law shown in Fig. 6. The DC motor armature voltage and the PVM voltage are shown in Fig. 11 and Fig. 12, respectively. The last one is $33.42V$ and the measured PVM current is $0.536A$; then, the PVM power is $17.91W$.

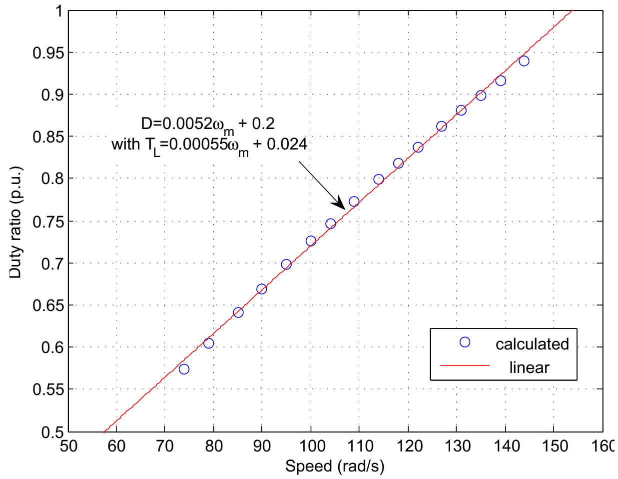

Fig. 6. Duty Cycle vs Maximum Motor Speed

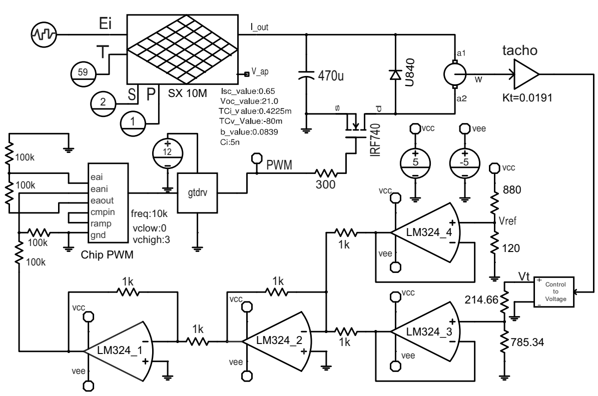

Fig. 7. Circuit implemented

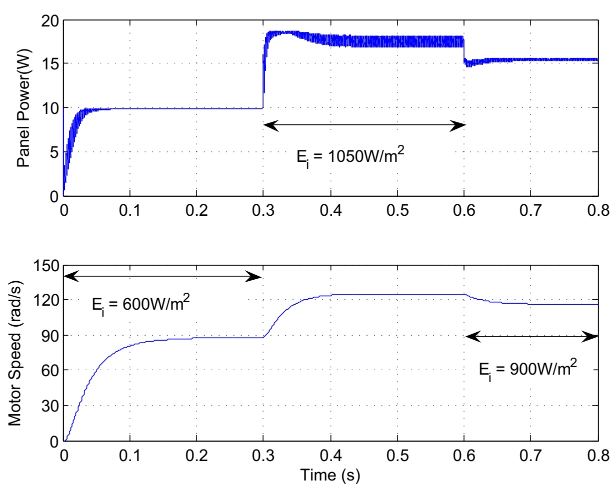

Fig. 8. Panel Power and Motor Speed

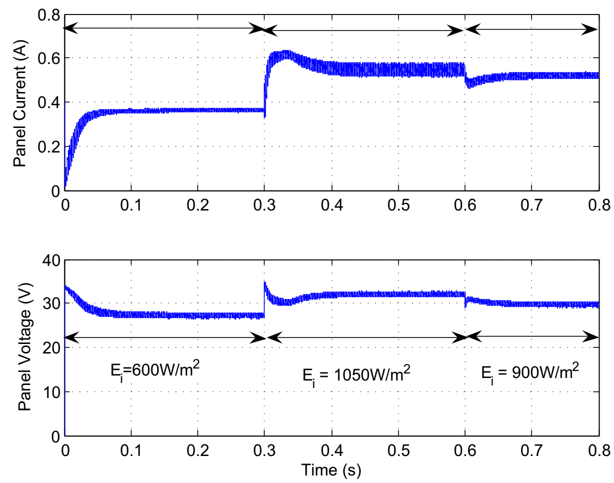

Fig. 9. Panel Current and Voltage

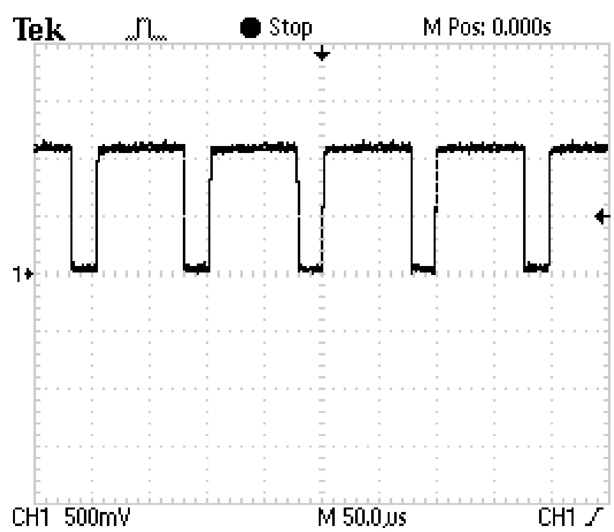

Fig. 10. Experimental waveform of PWM signal

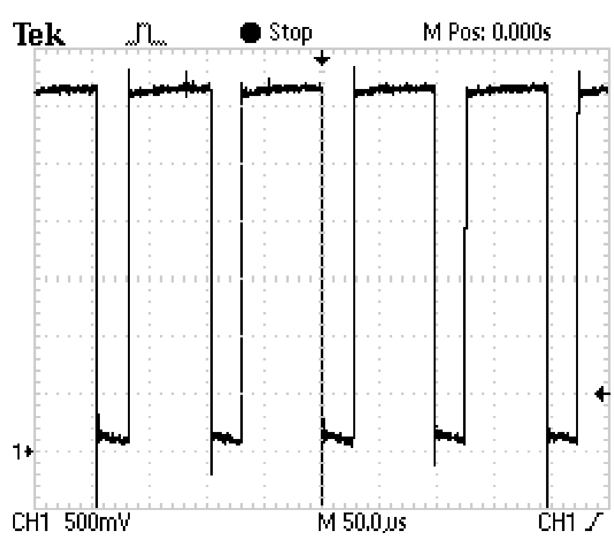

Fig. 11. Experimental waveform of armature voltage

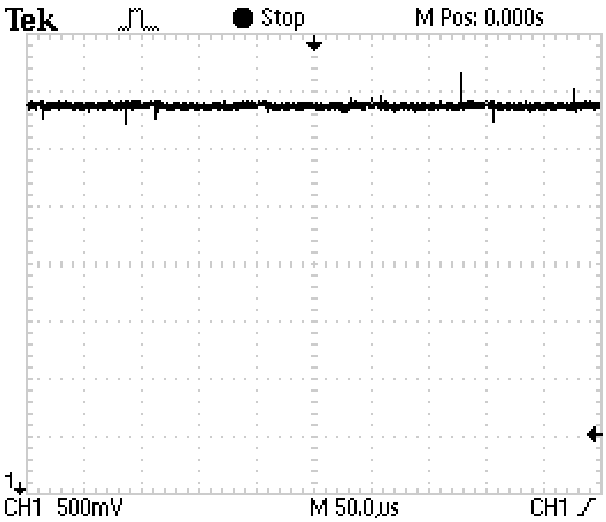

Fig. 12. Experimental waveform of PVM voltage

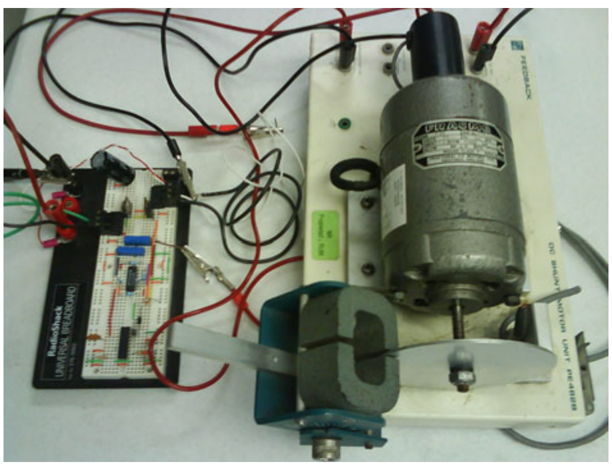

Fig. 13. Experiment Setup

V. Conclusion

This paper showed that it is possible to track the maximum power at different irradiance levels using a buck chopper and positive feedback of speed, only measurement speed is required. Also, it showed the necessary conditions for matching a PVM to a DC motor applying a step-down converter.

Using the mathematical model of PVM and DC motor, a control law relating the duty cycle of the chopper could be derived for a particular type of load. The control law is easily implementable using a cheap analog circuit composed of operational amplifiers and a PWM chip.

Acknowledgment

The authors gratefully acknowledge the contributions of all the members that belong to the Mathematical Modeling and Control of Renewable Energies for Advance Technology & Education ($M^2{}_{inds}$ CREATE) Research Team at UPRM. This project is sponsored by UPRM College of Engineering and General Motors PACE Program.

Also, special thanks to Dr. Gerson Beauchamp for allowing the use of the facilities in the Instrumentation and Control laboratory at UPRM.

References

[1] M. Ropp, *Encyclopedia of Energy Engineering and Technology*. CRCPress: Taylor and Francis Group, LLC, 2007, vol. 3, ch. Photovoltaic Systems, pp. 1147–1159.

[2] G. Masters, *Renewable and Efficient Electric Power Systems*. John Wiley & sons, Inc., 2004.

[3] S. Alghuwainem, "Steady-state performance of dc motors supplied from photovoltaic generators with step-up converter," *Energy Conversion, IEEE Transaction on*, vol. 7, no. 2, pp. 267–272, Jun 1992.

[4] ——, "Matching of a dc motor to a photovoltaic generator using a step-up converter with a current-locked loop," *Energy Conversion, IEEE Transaction on*, vol. 9, no. 1, pp. 192–198, Mar 1994.

[5] W. Fam and M. Balachander, "Dynamic performance of a dc shunt motor connected to a photovoltaic array," *Energy Conversion, IEEE Transaction on*, vol. 3, no. 3, pp. 613–617, Sep 1988.

[6] M. Saied, "Matching of dc motors to photovoltaic generators for maximum daily gross mechanical energy," *Energy Conversion, IEEE Transaction on*, vol. 3, no. 3, pp. 465–472, Sep 1988.

[7] ——, "A study on the matching of dc motors to photovoltaic solar arrays," *Electrical Machines and Systems, 2001. ICEMS 2001. Proceedings of the Fifth International Conference on*, vol. 1, pp. 652–655 vol.1, 2001.

[8] J. Appelbaum and S. Singer, "Magnification of starting torques of dc motors by maximum power point trackers in photovoltaic systems," *Energy Convers. Eng. Conf., IECEC-89., Proc. of 24th Intersociety*, pp. 749–754 vol.2, Aug 1989.

[9] S. Singer and J. Appelbaum, "Starting characteristics of direct current motors powered by solar cells," *Energy Conversion, IEEE Transaction on*, vol. 8, no. 1, pp. 47–53, Mar 1993.

[10] S. Shokrolla, N. Twieg, and A. Sharaf, "A photovoltaic powered separately excited dc motor drive for rural/desert pump irrigation," *Electrical Machines and Drives, 1993. 6th International Conf. on*, pp. 406–411, Sep 1993.

[11] K. Venkatesan and D. Cheverez-Gonzalez, "Matching dc motors to photovoltaic generators for maximum power tracking," *Applied Power Electronics Conf. and Exp. APEC '97 Conf. Proc. 1997., 12th Annual*, vol. 1, pp. 514–519 vol.1, Feb 1997.

[12] A. Tariq and M. Asghar, "Matching of a separately excited dc motor to a photovoltaic panel using an analog maximum power point tracker," *Industrial Technology, 2006. ICIT 2006. IEEE International Conf. on*, pp. 1020–1025, Dec. 2006.

[13] A. Sharaf and L. Yang, "A novel maximum power trecking controller for a stand-alone photovoltaic dc motor drive," *Electrical and Computer Engineering, 2006. CCECE '06. Canadian Conference on*, pp. 450–453, May 2006.

[14] A. Sharaf, E. Elbakush, and I. Altas, "An error driven pid controller for maximum utilization of photovoltaic powered pmdc motor drives," *Electrical and Computer Eng., 2007. CCECE 2007. Canadian Conf. on*, pp. 129–132, April 2007.

[15] E. Ortiz-Rivera and F. Peng, "Analytical model for a photovoltaic module using the electrical characteristics provided by the manufacturer data sheet," *Power Electronics Specialists Conf., 2005. PESC '05. IEEE 36th*, pp. 2087–2091, Sept. 2005.

[16] E. rtiz Rivera and F. Peng, "A novel method to estimate the maximum power for a photovoltaic inverter system," *Power Electronics Specialists Conf., 2004. PESC 04. IEEE 35th Annual*, vol. 3, pp. 2065–2069 Vol.3, 20-25 June 2004.

[17] O. Gil-Arias and E. I. Ortiz-Rivera, "A general purpose tool for simulating the behavior of pv solar cells, modules and arrays," *Control and Modeling for Power Electronics, 2008. COMPEL 2008. 11th Workshop on*, pp. 1–5, Aug. 2008.